ARTICLE TYPE www. rsc.org/xxxxxx | XXXXXXXX

A phenomenological theory of nonphotochemical laser induced nucleation

Marco Nardone[*a] **and Victor G. Karpov**[b]

Received Xth XXXXXXXXXX 20XX, Accepted Xth XXXXXXXXX 20XX
First published on the web Xth XXXXXXXXXX 200X
DOI: 10.1039/b000000x

We present a theory of electric field driven phase transitions that occur via nucleation of needle-shaped, metallic particles. The predictions of this theory have much in common with the observations related to nonphotochemical laser induced nucleation (NPLIN). That connection is rather paradoxical because the final NPLIN products are dielectric crystals. By elaborating on the unique features of field induced transitions and the complexities of liquid systems, we discuss how our theory may provide some insight to the open question of the NPLIN mechanism. A qualitative description of the post nucleation stage and conjectures about the microscopic nature of the metallic particles in liquids are also provided.

1 Introduction

Electric field induced nucleation (FIN) is a recently developed concept of needle-shaped, metal particle nucleation in an insulating host under a strong static [1,2] or oscillating (laser) [3] electric field (fields are typically in the range of $E \gtrsim 10^6$ V/m). Field induced transitions are observed in many technologically important areas, such as laser induced phase transformations in chalcogenide alloys [1] [underlying optical disc (DVD) recording], and electric bias induced transformations in the same materials [serving as a base for the phase change memory (PCM) technology], as well as bias induced insulator/conductor transformations in vanadium dioxide (VO_2) and other materials (with applications in optical and electric switches) [4–6]. A few common features of these transitions include: exponentially accelerated nucleation rates in the presence of the field; anisotropy that favors new phase growth in the direction parallel to the field; and a threshold field below which the anisotropic nucleation is not observed.

All of the above cases involve solids that undergo insulator-metal transitions. However, there is growing experimental support for electric field induced nucleation of solute particles in supersaturated solutions and other liquid systems (e.g. super-cooled liquids). First reported by Garetz et. al., [7] the phenomenon referred to as nonphotochemical laser induced nucleation (NPLIN) has been observed with both oscillating [7–19] and static [20] fields. The term 'nonphotochemical' emphasizes that there is no light absorption; hence, underlying changes in electronic structure capable of chemical reactions are ruled out. Clear indications, in many cases, that the field is the primary phase change driver are the alignment of nucleated particles along the direction of the applied field (or laser beam polarization) and the existence of a threshold field. It has led to a type of 'polarization switching' wherein the polymorph (crystal structure) of the nucleated crystal can be controlled by applying either linear or circular polarized light. [8,10] The underlying mechanism remains an open question with many practical implications. [21]

Although the NPLIN observations display the common features of FIN, a paradoxical issue is that the NPLIN experiments conducted to date have produced only dielectric crystals as the final product. The similarities between the predictions of FIN and the NPLIN observations has inspired the present work. Here we provide a theoretical basis for FIN in liquid systems but we restrict our analysis to systems that are capable of a metal phase since it is not clear how the dielectric products of the NPLIN experiments are manifested.

A significant insight of FIN theory is that, when the electric field is strong enough, the energy reducing effect of the elongated conductive particles allows metals to form even when the metallic phase would be unstable in the absence of the field. That leads to intriguing predictions, such as the formation of metals at unexpected temperatures and pressures, or field induced nucleation of *dielectric* particles via short-lived metallic precursors. We elaborate on the latter possibility below by presenting a summary of the available data on NPLIN of dielectric crystals and discussing how the theory described herein may shed some light on the underlying mechanism.

Recent observations of laser-induced water condensation in air [22] may also be connected with FIN. In that work, water condensation in the sub-saturated atmosphere was induced by ionized filaments generated by ultra-short laser pulses. The

[a] *Department of Environment and Sustainability, Bowling Green State University, Bowling Green, OH 43403, USA. E-mail: marcon@bgsu.edu*
[b] *Department of Physics and Astronomy, University of Toledo, Toledo, OH 43606, USA.*

nucleation mechanism is not known but it is clear that the laser field causes a phase transition to a dielectric product (water) via an electrically conductive plasma. In that case, however, the laser intensity is approximately two orders of magnitude larger than in the NPLIN experiments leading to multiphoton ionization of air molecules; hence, photochemical effects become important.

It is worth noting that similar effects of the electric field on material structure have been observed independently for a variety of glassy systems. This includes exponentially strong increase in nucleation rates,[23] the intriguing phenomenon of the alignment of nucleated (crystal) particles to the laser beam polarization,[24,25] and threshold nature of nucleation vs. laser beam intensity.[26] The underlying mechanisms remain largely unknown. It was however realized that the electric field induced reduction in the nucleation barrier could be qualitatively attributed to the field induced polarization of spherical embryos whose induced electric dipoles interact with the field; this was described in the framework of the classical nucleation theory.[23] In general, it is natural to assume that the observed similarity of the field induced transformations in NPLIN and glassy systems is due qualitatively to the same phase change mechanism.

The latter approach based on the classical nucleation theory was considered for NPLIN of dielectrics as well.[13–15] As described in detail in Sec. 6, this explanation leads to a correct qualitative prediction of the nucleation barrier decreasing linearly with laser power, in agreement with the observations. However, the corresponding field-driven barrier reduction, ΔW, turns out to be five orders of magnitude below the observed effect (predicting, say, $\Delta W \sim 0.003kT$ instead of the observed $30kT$).

Our paper is organized as follows. Section 2 describes the known theoretical results[13–15,23] of the electric field effect on nucleation of spherical dielectric particles. We show which physical parameters make that effect small compared to the electric field induced barrier reduction that can be achieved by needle-shaped metallic particles. In Sec. 3 we describe a more quantitative theory of field induced nucleation that provides numerical estimates sufficient for comparison with the experimental data. Sec. 4 concentrates on the post-nucleation stage and the related peculiarities of field induced nucleation in solutions. In Sections 2-4, the microscopic structure of the metallic particles remains arbitrary. Therefore, Sec. 5 is devoted to the question of conceivable microscopic models; several such models are discussed. Finally, Sec. 6 provides a general discussion including a summary of the experimental data for NPLIN of dielectric crystals and how our results may help to elucidate the underlying mechanism, along with possible methods of experimental verification.

2 Qualitative analysis

The following provides a qualitative comparison of the field effects predicted by classical nucleation theory and nucleation in a symmetry-breaking electric field. We show that nucleation of spherical particles cannot account for the often observed dramatic field effects.

2.1 Field effect in the classical nucleation theory

The classical nucleation theory[27,28] assumes spherical nuclei that are described by the coefficient of surface tension σ and the chemical potential difference (per volume) between the two phases μ. Their free energy in zero field is given by

$$F = A\sigma - V\mu,$$

where the surface area is $A = 4\pi R^2$, and the nucleus volume is $V = (4/3)\pi R^3$. This leads to the well known results for the classical barrier and critical radius given respectively by

$$W_0 = 16\pi\sigma^3/(3\mu^2) \quad \text{and} \quad R_0 = 2\sigma/|\mu|.$$

The sign in absolute value of the last formula does not affect the classical definition of R_0; however, it enables one to extend that definition to the case of energetically unfavorable bulk phases that will be shown to result form needle-shaped particles under strong enough electric field (Sec. 2.2, 3). For the case of solutions, the chemical potential can be approximated as $\mu = kT \ln s$, where s is the supersaturation.

The field effect is accounted for by the electrostatic contribution to the free energy originating from the interaction $-pE$ of the particle's induced electric dipole $p \propto E$ with the field E. A particle of generic shape and volume V in a uniform field E reduces the free energy according to,[29]

$$F_E = -\frac{\varepsilon^* E^2}{8\pi} V \quad \text{with} \quad \varepsilon^* = \frac{\varepsilon\Delta\varepsilon}{\varepsilon + n\Delta\varepsilon}. \tag{1}$$

Here, the particle polarizability depends on the effective permittivity, ε^*, which in turn is a function of the difference $\Delta\varepsilon = \varepsilon_p - \varepsilon$ between the particle (ε_p) and host (ε) permittivities and the shape of the particle through the depolarizing factor, n. The latter equals $1/3$ for the case of sphere. As a result, for a dielectric sphere of permittivity ε_p in a host with permittivity ε, we have

$$\varepsilon^* = 3\varepsilon(\varepsilon_p - \varepsilon)/(\varepsilon_p + 2\varepsilon). \tag{2}$$

Adding the contribution in Eq. (1) and assuming that the particle shape remains spherical results in the effective renormalization of the volume term (proportional to V) in the free energy,

$$F = A\sigma - V\mu + F_E. \tag{3}$$

Therefore, the optimization procedure remains the same yielding the nucleation barrier $W_{sph} = \max\{F(R)\}$ and its corresponding critical radius in the form

$$W_{sph} = \frac{W_0}{\left(1 + E^2/E^{*2}\right)^2} \quad \text{with} \quad E^* = 2\sqrt{\frac{3W_0}{\varepsilon^* R_0^3}}, \qquad (4)$$

$$R_{sph} = \frac{R_0}{1 + E^2/E^{*2}}. \qquad (5)$$

Here E^* has the meaning of the characteristic field above which the field effect on nucleation becomes strong. Note that the critical radius and the nucleation barrier in the field are smaller than their respective zero-field values when $\varepsilon_p > \varepsilon$; hence, the nucleation rate increases.

The above effect tends to be rather insignificant in the case of dielectric sphere nucleation. Consider a scenario where the observed field induced barrier reduction is $\Delta W = 30kT$. From Eq. (1), setting $F_E = \Delta W$ yields $\varepsilon^* = 8\pi\Delta W/(E^2 V)$. As a rough estimate, a particle of volume $V \sim R_0^3 \approx 3$ nm^3 and an applied field of $E \sim 10^7$ V/m gives the requirement $\varepsilon^* \sim 10^4$. In comparison, for a dielectric sphere we have Eq. (2) with $\varepsilon_p = 2.2$ (e.g. for KCl) and $\varepsilon = 1.8$ (for water in a laser field of wavelength $\lambda = 1.064\ \mu$m),[30] yielding $\varepsilon^* = 0.4$; five orders of magnitude too low. One could arrive at the same conclusion based on the estimate of $E^* \sim 10^{10}$ V/m obtained by substituting the above numerical parameters in the definition of E^* in Eq. (4). When $E^* \gg E$, it follows from Eq. (4) that the expected field effect is negligibly small for the typical experimental conditions discussed in Sec. 6. These qualitative estimates reveal the unlikelihood that a dielectric particle could provide the necessary barrier suppression.

To reinforce the above claims, we also provide the following very rough but indispensable argument. Taking into account that the induced dipole is $p = \beta E$ where β is polarizability and requiring a field effect of $pE \sim 30kT$ at room temperature, one arrives at $\beta \sim 10^{-17}$ cm^3. Since it is known that the polarizability of a spherical metal particle of radius R is $R^3/2$, one arrives at the conclusion that *metallic* particles of radius greater than 10 nm are needed to account for the energy reduction (or much larger dielectric particles), which is well beyond the known range of nucleation radii.

The above results can be interpreted as evidence of the insufficient polarizability predicted by the classical nucleation theory. Therefore, in what follows we will concentrate on modifications that can significantly increase the polarizability of a new phase particle: metallic nature, and needle-like elongated shape. This is qualitatively discussed in the next subsection.

2.2 Needle-shaped metallic particles

A relevant case of gigantic polarizability is found with a metal needle of length H and radius $R \ll H$. Under an electric field E, it will accumulate at its ends opposite charges of absolute value $q \sim EH^2\varepsilon$ corresponding to the dipole moment $p_m \sim qH = EH^3\varepsilon = E\varepsilon V(H/R)^2$, where ε is the dielectric permittivity of the host material and $V \approx HR^2$ is the particle volume. For comparison, a spherical dielectric particle of equal volume and characteristic dimension $V^{1/3}$ will develop, under the same field, the dipole moment $p_d \sim E\Delta\varepsilon V \ll p_m$, where $\Delta\varepsilon = \varepsilon_p - \varepsilon \ll \varepsilon$. Hence, the electrostatic energy gain in nucleation, pE, is higher for needle-shaped metal particles by approximately a factor of $(\varepsilon/\Delta\varepsilon)(H/R)^2 \gg 1$.

It is remarkable that under strong enough fields, the above estimate predicts stable, needle-shaped metallic particles even when their constituting bulk phase is energetically unfavorable. Indeed, the above electrostatic energy gain $\sim E^2H^3$ will overbalance the chemical potential loss $|\mu|R^2H$ when $E \gg (R/H)\sqrt{|\mu|}$ for high aspect ratio shapes with $R/H \ll 1$. In other words, nucleation of an energetically unfavorable metallic phase can occur that is totally forbidden by the classical nucleation theory. Physically, this enhancement is due to a large induced electric dipole in the needle-shaped particle. Once created, it will act as a lightning rod, concentrating the field and triggering further nucleation.This energy analysis will be made more quantitative in Sec. 3 below.

Regarding the dynamic characteristics in a laser field, we note that the typical metal plasma frequency in the range of $\omega_p \sim 10^{15} - 10^{16}$ s^{-1} is much greater than both the typical applied laser frequencies and the characteristic dielectric relaxation frequencies corresponding to reorganization and orientation of permanent dipoles, which are all below $\omega_d \sim 10^{11}$ s^{-1}. Therefore, the metal particles will behave as good metals in the laser field.

Two comments are in order regarding the above consideration. The first addresses the commonly known trend that metallic properties are suppressed when the particle size decreases. Taken superficially, that trend may seem to undermine the assumption of small metal nuclei. We note, however, that the nature of that trend is dimensional quantization:[31] the metallic properties disappear when the characteristic dimensional quantization energy gap $E_a \approx \hbar^2/ma^2$ in a particle of size a becomes greater than the thermal energy kT. This would change the nature of the electronic spectrum from an effectively continuous ($E_a \ll kT$) metallic type to the discrete spectrum typical of dielectrics. It is readily seen, however, that such quantization does not take place because the needle-shaped nuclei can be sufficiently long.

As an example, a nano-size particle ($a = 1$ nm) with the electron mass $m \sim 10^{-27}$ g corresponds to an energy gap $E_a \sim 0.1$ eV, too wide to maintain metallic properties. We will see in what follows that the needle-shaped nuclei considered here typically have transversal dimension (R) on the scale of 1 nm and, therefore, detrimental to metallic conductance. However, their longitudinal dimensions (H) are much greater, say

$H \sim 10$ nm, leading to energy gaps of $E_a \sim 0.001$ eV, fully consistent with the notion of metal conduction. In that case, typical of highly anisotropic systems, the metallic properties are due to the quasi-continuous, possibly overlapping energy sub-bands related to the longitudinal dynamics (we assume that the Fermi level lies in one of those sub-bands).

Our second comment addresses the characteristic time necessary to form a metal cluster during the duration of one laser pulse, $\Delta t \sim 10$ ns. Bearing in mind the needle-like shape of the particles and limiting the transport to diffusion only, the criterion of fast enough nucleation kinetics is that atomic particles can diffuse distances of the order of R, i. e.

$$4D\Delta t \gtrsim R^2$$

where D is the diffusion coefficient and the coefficient of 4 accounts for the 2D (perpendicular to the cylinder axis) diffusion component. Using for specificity a reasonable values of $D = 2.1 \times 10^{-9}$ m^2/s and $\Delta t \sim 10$ ns shows that the latter criterion holds up to a radius of 10 nm. Therefore, field induced nucleation is not inhibited by low atomic diffusivity: metallic nuclei have time to form during a single laser pulse of 10 ns. Alexander et. al.[13] arrived at the same conclusion for dielectric clusters.

3 Field induced nucleation

3.1 Field dependent nucleation barrier for needle-shaped particles

The above claim of strong energy gain can be made more quantitative in the framework of field induced nucleation (FIN) theory.[1–3] FIN is a recently developed concept of metal phase nucleation in an insulating host under a strong static[1] or oscillating[3] field. In particular, we explicitly show next how phase transitions are possible even for the case of an energetically unfavorable bulk new phase (negative μ) when a strong electric field is applied and the constraint of spherical shape is relaxed.

We start with noting that the equilibrium form of a particle in a uniform field is close to prolate spheroidal.[32] Referring then to Eq. (1) we use the depolarizing factor for a prolate spheroid of radius R and height H, given by[29]

$$n = (R/H)^2[\ln(2H/R) - 1]. \quad (6)$$

From Eq. (1), a metallic particle with $\varepsilon_p \to \infty$ leads to $n\Delta\varepsilon \gg \varepsilon$, resulting in $\varepsilon^* = \varepsilon/n$, consistent with the intuitive estimate presented in Sec. 2.2 for the dipole moment, p_m, of a metallic needle. At optical frequencies, where ε_p is finite and negative, the polarization enhancement is governed by plasmonic oscillations that are in resonance with the field frequency.[33] Rather than elaborating on the latter mechanism here, we simply mention that the plasmonic driven field-induced polarization can be larger in magnitude than that of a static field by the quality factor $Q = \omega\tau$, where ω is the laser frequency and τ is the electron relaxation time in the metallic phase. The corresponding nucleation barrier turns out to be lower by a factor of $1/Q$. However, the measured Q for metallic nanoparticles are not very large: the ratio of the plasmonic peak frequency over peak width is of the order of 3-5.[34] In what follows we will assume that factor is included in the parameter α, if necessary, in order to maintain simplicity of consideration.

For the case of needle-shaped particles, nucleation proceeds through two degrees of freedom by forming high aspect ratio metallic clusters aligned with the field (or laser beam polarization). They are efficient at reducing the electrostatic energy because of their larger dipole moments. Their exact shape is not known, but modeling with either spheroidal or cylindrical particles leads to differences only in numerical coefficients.[1] We opt for the mathematically more concise form of a cylindrical nucleus with $A = 2\pi RH$ and $V = \pi R^2 H$, leading to the free energy of Eq. (3) expressed as,

$$F_{cyl} = \frac{W_0}{2}\left(\frac{3RH}{R_0^2} \pm \frac{3R^2H}{R_0^3} - \frac{E^2}{E_0^2}\frac{H^3}{R_0^3}\right). \quad (7)$$

Here we have assumed the particle to be metallic with $\varepsilon^* = \varepsilon/n$ and used the approximation $n = (R/H)^2$, thereby setting the expression in the square brackets of Eq. (6) to unity. In the second term of Eq. (7), we allow μ (included in R_0) to be negative for a new phase that is energetically unfavorable in the bulk. Here, the characteristic field is given by,

$$E_0 = 2\sqrt{\frac{W_0}{\varepsilon R_0^3}}. \quad (8)$$

The contour plot in Fig. 1 illustrates how the system can lower its free energy more easily by forming elongated particles. We note that the zero-energy contour (labeled 0) in Fig. 1 represents the boundary beyond which the free energy is negative. It is defined by the equation,

$$\frac{H}{R} > \sqrt{3\left(1 + \frac{R_0}{R}\right)}\frac{E_0}{E}, \quad (9)$$

consistent with our above qualitative conclusion about the possibility of needle-shaped particles of an otherwise energetically unfavorable phase.

We now turn to the question of the nucleation barrier corresponding to FIN. The free energy of Eq. (7) seems to suggest that nuclei with $R \to 0$ are the most favorable. Realistically, R must be greater than some minimum value determined by extraneous requirements, such as sufficient conductivity to support a large dipole energy or mechanical integrity. Based on

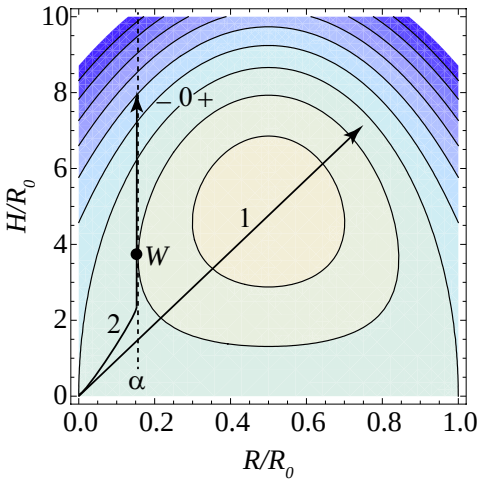

Fig. 1 Contours of free energy F/W_0 from Eq. (7); positive and negative regions are separated by the zero contour. The contour spacing is $F/W_0 = 0.5$. Nucleation of elongated particles along path 2 over the barrier W is more efficient than nucleation over the maximum barrier of path 1. $R/R_0 = \alpha$ is the minimum physically reasonable radius.

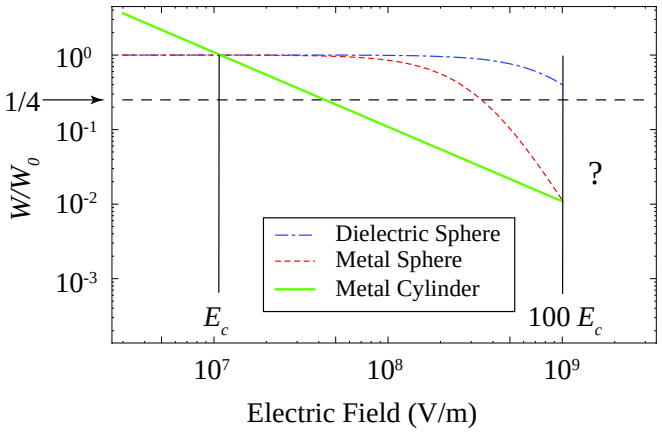

Fig. 2 Comparison of the field induced barrier suppression from Eqs. (4) and (10) for a dielectric sphere (dash-dot), metallic sphere (dash), and metallic cylinder (solid). Experimentally observed barrier reduction $W/W_0 = 1/4$ (with $W_0 = 40kT$), shown by the horizontal line, is achieved near 3×10^7 V/m for the metallic cylinder; in the range the data (see Sec. 6). The region $E_c < E < E_c/\alpha^2$ (using $\alpha = 0.1$) is the effective range of FIN. Nucleation in the region $E > E_c/\alpha^2$ is uncertain due to the requirement of ultra-small nuclei. The numerical values are provided in the running text.

data for other types of systems, it was estimated[1] that a reasonable minimum radius is $R_{min} = \alpha R_0$, where $\alpha \sim 0.1$ is a phenomenological parameter. Assuming R_0 of several nanometers puts R_{min} in the molecular size range. Lacking more concrete information, we employ the same approximation here. In the region $R < R_{min}$, the free energy is substantially larger than described by Eq. (7), since the energy reducing effect of the electric field cannot be manifested by such thin particles. The region $R < R_{min}$ can be approximated by a potential wall.

Following previous work,[1] we consider nucleation along the path $R/R_0 = \alpha$ (see Fig. 1); alternative paths that start from the origin introduce only insignificant numerical factors. Then, from Eq. (7), the nucleation barrier and critical aspect ratio are,

$$W = W_0\frac{\alpha^{3/2}E_0}{E} \equiv W_0\frac{E_c}{E}, \quad \frac{H_c}{R_{min}} = \frac{E_0}{\alpha^{1/2}E} \gg 1 \qquad (10)$$

to within the accuracy of insignificant numerical multipliers of the order of unity. Here E_c is the characteristic field, above which FIN dominates. Employing typical nucleation values of $W_0 \sim 1$ eV, $R_0 \sim 3$ nm, and $\alpha \sim 0.1$, Eq. (10) predicts that a substantial barrier reduction is achieved at a field of $E \gtrsim E_c \sim 10^7$ V/m for metallic cylinders; within a reasonable experimental field range. In a static field, we have $\varepsilon \sim 100$ for aqueous solutions and the latter value is reduced to $E_c \sim 10^6$ V/m. The field dependent nucleation barriers for various scenarios are shown in Fig. 2.

Comparing Eqs. (4) and (10) indicates that nucleation of needle-shaped particles is favored when $W < W_0$, resulting in the critical field condition $E > E_c \equiv \alpha^{3/2}E_0$. The requirement on the aspect ratio $H_c/R_{min} \gg 1$ from Eq. (10) implies the upper limit $E < E_0/\sqrt{\alpha}$. Taken together, FIN is effective in the range,

$$1 < E/E_c < \alpha^{-2}, \qquad (11)$$

which is clearly indicated in Fig. 2; $10^7 < E < 10^9$ V/m for the numerical values mentioned above. Beyond the upper limit ($E > E_c/\alpha^2$), small nuclei with $R < R_{min}$ are expected. The nucleation of such small particles can involve other physical aspects[35] that we do not consider here. Below the field range, spherical particles may be more probable than cylinders but the field effect is negligible (i.e. insignificant barrier suppression).

3.2 FIN in the proximity of bulk phase transitions and the threshold laser power

Another interesting observation concerns the dominance of FIN near bulk phase transition ($\mu \approx 0$), such as solid-liquid, metal-dielectric, etc. To account for the bulk phase transition, one can use the standard approximation $\mu = \mu_0\Theta$ where Θ is the phase transition parameter and μ_0 is the chemical potential difference between the two phases at $\Theta = 1$. For example, $\Theta = |1 - T/T_c|$ for phase transitions described by a critical temperature, T_c (e.g., in the metal-dielectric transition of VO_2).

For the case of solutions we quantitatively define supersaturation as $s = (c/c_0) - 1$ to make it formally similar to the case

of temperature (note that some sources[13] use the definition $s = c/c_0$). We then take into account that the difference in chemical potentials between the actual and oversaturated solutions is proportional[36] to s. Because the chemical potentials of the oversaturated solution and material in the second phase coincide, one can write $\mu \propto \Theta = s$.

The latter relation will result in a corresponding renormalization, according to which the above introduced parameters will be replaced respectively by the following,

$$W_0 \to \frac{W_0}{\Theta^2}, \quad R_0 \to \frac{R_0}{\Theta}, \quad E_0 \to E_0|\Theta|^{1/2}. \qquad (12)$$

Because $R_{min} = \alpha R_0$ is determined by microscopic structure and remains practically independent of Θ, we observe that $\alpha \propto \Theta$. Taking into account the latter scaling relations, Eq. (10) predicts that the nucleation barrier W is Θ-independent.

This conclusion is in striking difference with the prediction of classical nucleation theory that the nucleation barrier for spherical embryos is strongly Θ-dependent,

$$W_0 \propto \Theta^{-2}. \qquad (13)$$

This prediction[6] was recently compared to experimental data for the case of FIN in VO_2.

It is readily seen from the above that FIN of needle-shaped embryo becomes exponentially more effective than the classical nucleation of spherical particles in the proximity of the bulk phase transition. Indeed, the latter is characterized by the barrier that can be presented as $W_0 = W_{00}\Theta^{-2}$ while the Θ-independent field induced nucleation barrier can be presented in the form $W = W_{00}\alpha_{00}^{3/2}E_{00}/E$, where W_{00}, E_{00}, and α_{00} refer to $\Theta = 1$. As a result, field induced nucleation can dominate under relatively weak fields $E > E_{00}\alpha_{00}^{3/2}\Theta^2$ near the phase transition point. Here, the characteristic values of the "zero temperature" quantities W_{00}, E_{00}, and α_{00} far from the bulk phase transition are estimated in the above as their respective values without indices: W_0, E_0, and α. Simply stated, FIN is prevalent in the proximity of bulk phase transitions; the required electric fields can be either externally applied, say, in the form of low power laser beam, or generated internally as a result of minute material nonuniformities.

In the framework of FIN theory, the time of the experiment (i.e., the duration of field exposure Δt) can play a significant role determining the threshold field, below which field induced nucleation becomes unlikely. This relation is based on the understanding that the exposure time must be greater than the nucleation induction time $\tau = \tau_0 \exp(W/kT)$ with W from Eq. (10). Equating $\Delta t = \tau$ gives the threshold field,

$$E_{th} = \frac{W_0}{kT}\frac{E_c}{\ln(\Delta t/\tau_0)}, \qquad (14)$$

where k is Boltzmann's constant and T is temperature. This provides verifiable predictions in terms of the threshold field dependence on exposure time, temperature, and the supersaturation s.

One non-trivial prediction from Eq. (14) is that the threshold field (or threshold laser power density) does not depend on the order parameter Θ, in particular, E_{th} does not depend on supersaturation for the case of FIN in solutions. This prediction is fully consistent with the available data,[13] and cannot be explained by the classical nucleation theory.

Furthermore, assuming reasonable $\ln\Delta t/\tau_0 \sim 10$, $W_0/kT \sim 30$, and $E_c \sim 10^7$ V/m (see Fig. 2) yields $E_{th} \sim 3E_c$. This translates into the threshold laser power $I_{th} = cE_{th}^2/(4\pi) \sim 100$ MW/cm^2, where c is the speed of light. The prediction of the threshold field and laser power being logarithmically dependent on the time of exposure, Δt, calls upon experimental verification.

4 Post-nucleation kinetics

The above analysis was limited to the nucleation stage of the phase transformation. That limitation is well justified in some cases. For example, field induced nucleation in chalcogenide glasses results in metallic embryos of crystalline structure that are stable enough and can exist as such for a long time.[1–3,24,25] However, post-nucleation growth (or decay) can strongly affect the number of experimentally observed second phase particles in many other systems. In general, the post-nucleation processes can be rather complex, including secondary nucleation of the second phase particles on precursor embryos, structural reconstruction,[37] and subsequent particle growth by accretion from the solution. The reconstruction step implies that "nucleation is, at least, a two-barrier process in terms of the thermodynamic potential, in which the first barrier necessary for cluster formation is lower than the main barrier necessary for the transformation of the already formed cluster into a stable crystalline nucleus";[37] it goes beyond classical nucleation theory and was suggested based on empirical observations.

A possible complication that is characteristic of field induced nuclei is that they remain stable when a strong enough electric field is present and thus become strongly unstable (left with significant excessive free energy) upon field removal. This instability can result in extremely rapid decay accompanied by substantial volume and temperature changes, and pressure gradients conducive of local shock waves and cavitation. The latter factors can by themselves serve as important phase transformation drivers.[17,18,38] Since this scenario is extremely difficult to describe theoretically, we leave it here as a possibility that cannot be ruled out. We note, however, that the scenario can hardly work for the cases of nucleation under dc field or laser-induced phase transformations in glassy systems.[24,25] In what follows, we attempt a semi-quantitative descrip-

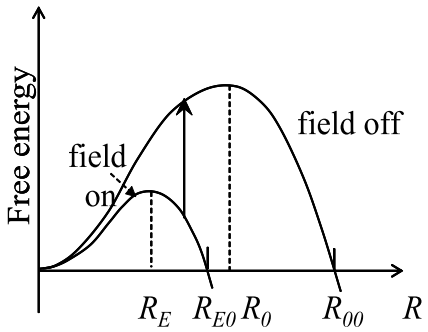

Fig. 3 Sketch of the particle free energy under zero field and strong electric field. R_0 and R_E show the corresponding nucleation barriers, while R_{00} and R_{E0} represent the radii above which the particle becomes energetically favorable. The upward arrow shows the transition that takes place upon field removal, which leads to particle decay.

tion of how the secondary process depends on the field and solute concentration for the standard scenario of post-nucleation kinetics.

As illustrated in Fig. 3, a newly nucleated particle will remain unstable upon field removal unless it grows enough ($R > R_0$ in Fig. 3) to ensure particle stability (continued growth) in zero field. Therefore, the field needs to be maintained for a sufficient time to let a just nucleated particle evolve into the zero-field stability region. The particle growth rate determines both that time and the number of stable particles found upon field removal. Assuming the characteristic time of field exposure Δt, the condition of sufficient growth takes the form $R(t = \Delta t) > R_0$.

When the post-nucleation stage of particle formation becomes the bottleneck, the phase transformation rate will not be exponential in the electric field and material parameters, as would be typical for nucleation processes.[28] Here, we consider a conceivable scenario that is unique to the field induced mechanism and is inspired by the NPLIN data (see Sec. 6).[8,13] Since the field greatly increases the nucleation rate, we assume the growth stage to be the bottleneck that determines the number of particles observed upon field removal, while the characteristic nucleation time $\tau \ll \Delta t$ is the shortest of all the processes. Thus, metal nucleation takes place with certainty during the time Δt of field exposure. Therefore, the number of particles to grow beyond the stability radius R_0 is proportional to the diffusion flux I of molecules from the solute to the particle. The latter is given by the equation,[36]

$$I = 4\pi r^2 D\, dc/dr = 4\pi D(c - c_{0\infty})(R_0 - R_E), \qquad (15)$$

where we have implied a spherical nucleus with radius close to the critical radius R_0, c is the solute concentration, and $c - c_{0\infty} \equiv \Delta c$ is the solute over-saturation. Because the practical fields are much lower than E_*, it follows from Eq. (5) that $R_0 - R_E \approx 2R_0E^2/E_*^2$, which yields for the number of stable particles,

$$N \propto DE^2\Delta c. \qquad (16)$$

Obviously, E^2 should be replaced with the laser power for the case of laser fields. The dependence in Eq. (16) can be shown to hold not only for spherical particles [assumed in Eq. (15)], but for cylindrical particles as well (to within the accuracy of a numerical coefficient).

We conclude that, when the field is sufficient to induce nucleation of metallic particles ($E > E_c$), the probability of observing crystallization depends on the field and concentration according to Eq. (16); as observed in several of the NPLIN experiments[8,13,39] discussed below. The dependence on the diffusion coefficient D (which can be affected by temperature) remains to be verified. Another verifiable prediction is that shortening the laser pulses down to the sub-nanosecond range should suppress nucleation because of insufficient time to grow the needle radius beyond zero field stability value R_0 (see Fig. 3).

5 On the microscopic nature of metallic nuclei

In some cases, the nature of the predicted needle-shaped nuclei is well known. For example, they are metallic crystal particles in chalcogenide glasses. In general, however, we note that the field induced decrease in free energy [last term in Eq. (7)] may provide a means by which otherwise chemically unstable conductive particles can persist in an electric field when their aspect ratios exceeds that in Eq. (9). Here the phrase 'chemically unstable' corresponds to the case when the sign in front of the second term in Eq. (7) is positive. This opens intriguing possibilities for the metallic nature of the particles, a few of which are considered next.

Consider first the example of a pure metal, such as the violently reactive combination of potassium in water with an enthalpy of reaction, $\mathcal{H} \approx 200$ kJ/mol. We will take $\mathcal{H}$ as an approximation for the thermodynamic potential difference Φ, whose value per particle gives the chemical potential μ. In that case, using the standard potassium density of ≈ 0.86 g/cm^3 yields $\mu \sim 4$ kJ/cm^3. The latter suffices to estimate the characteristic field E_0 introduced in Eq. (8). Representing it as $E_0 = \sqrt{8\pi\mu}$ gives $E_0 \approx 5\times10^{10}$ V/m. Assuming, as in the above, $\alpha \sim 0.1$ yields then $E_c \sim 10^9$ V/m, much larger than the typical experimental fields of $E \sim 10^7$ V/m. Also, given a surface tension of $\sigma \sim 0.1$ J/m^2 for potassium,[40] the above estimated μ results in an unrealistic linear size scale of R_0 in the sub-angstrom range.

However, one can consider a metal phase of more complex nature than pure potassium and with substantially lower en-

thalpy of reaction. A set of useful hints towards such phases is found in the extensive work on the various scenarios of metal-insulator transitions; Mott[31] has given a comprehensive review of that field. Among such transformations, the case of insulator-to-metal transitions due to solvated electrons appears plausible in application to NPLIN; it is briefly described next.

The concept of solvated electrons, originally proposed for the case of metal (often K or Na) ammonia solutions, implies that the electron can form a localized state by self-consistently polarizing the surrounding medium, which, in turn, creates a potential well for the electron. Similar to the concept of polarons, it is made more specific by assuming that the required polarization is achieved via properly orienting NH_3 molecules possessing considerable dipole moments. This results in a cavity-like potential well confining the electron and having a depth of the order of the potential step through its surrounding dipole layer. The details of this picture were extensively discussed through both new experimental verifications, particularly including the cases of Na and K,[41] and mathematical treatments, as described in recent reviews.[42,43]

A feature of interest here is that the system of solvated electrons undergoes an insulator-to-metal transition when the concentration of solvated electrons exceeds a certain critical value in the range of 7-20 molar percent, above which the conductivity approaches values similar to that of liquid mercury. The transition is thought of as occurring through collectivizing of the solvent electron states with concomitant suppression of their surrounding dipole layers; various mathematical models were proposed.[44]

The above outlined concept of solvated electrons could be relevant for NPLIN of dielectrics, in particular, for K and Na solutions as containing those metals that are known to supply the solvated electrons with water being a source of electric dipole units. Other systems studied by Garetz et. al. can include significant fractions of strong electric dipole molecules facilitating the electron solvation, as suggested by their chemical formulas: histidine ($C_6N_3O_2H_9$), glycine (NH_2CH_2COOH), urea ($CO(NH_2)_2$), and lysozyme.

Our theory predicts that under a sufficiently strong field the insulator-to-metal transition in a system of solvated electrons will occur through nucleation of needle-shaped, metallic clusters. Quantitative estimates of the corresponding characteristic fields E_0 and E_c can be attempted based on the available information about the parameters of solvated electrons in metal ammonia solutions. Namely, the enthalpy of transition to the metallic state can be up to two orders of magnitude lower than that of the above discussed case of pure potassium (say,[45] $\mathcal{H} \approx 2$ kJ/mol). The corresponding characteristic field is $E_c \sim 5\times10^7$ V/m and using[31] $\sigma \sim 32$ erg/cm^2 yields $W_0 \sim 2$ eV and $R_0 \sim 2$ nm, consistent with the above theory.

Another possibly relevant mechanism of nonmetal-metal transitions[31] is related to noncrystalline semiconductors and impurity bands. The underlying model is that of localized electrons with localization radius a_l each at randomly positioned centers of concentration n_l. When the electron wave function overlap is significant enough, the participating states form an energy band that can give rise to metallic conduction. This kind of transition is well studied both theoretically and experimentally. The criterion of metal conductivity is that the volume fraction occupied by localized electrons is high enough, $n_l a_l^3 \gtrsim 0.005$.

While the concept of a band of free electrons in water remains largely unexplored,[47] one can consider electronic states localized at positively charged ions, such as potassium K^+, or hole states localized at negative ions, such as chlorine Cl^-. They can be thought of either as hydrogen-like states in semiconductors or as Frenkel-type excitons. Assuming their radii of the order of ~ 3 Å (typical of electrons in water[42,43,47]), the required concentration of such centers becomes of the order of 10^{21} cm^{-3}, i.e., ~ 3 atomic percent. The latter could be achieved, at least locally, with an average KCl solute concentration $\sim 10\%$. Overall, this microscopic mechanism of metal particle formation remains highly speculative.

6 Discussion and conclusions

The theory of field induced nucleation accounts for phenomena where an electrical bias causes phase transitions to occur exponentially more rapidly than predicted by classical nucleation theory. It has been applied to solid systems, such as metal-insulator transitions in chalcogenide alloys[1–3] and vanadium dioxide.[6] In the present work we have specifically considered FIN in liquid systems that are capable of metal nucleation in a laser or static field. We recall that a unique feature of FIN is that chemically unstable species may become stable as long as the field is present. The opportunity to form otherwise unstable, short-lived species and the complexity of solutions with high concentrations of solvated ions and electrons can lead to unanticipated phases and rich post-nucleation kinetics, as described in Sec. 4 and 5. As such, we discuss next how our theory may shed some light on the observed NPLIN of dielectric crystals.

6.1 Application to NPLIN of dielectric crystals

Our summary of NPLIN data from the literature is presented in Fig. 4 where the peak laser intensity (or applied field) and exposure time are provided at which crystallization was eventually observed in solutions at various supersaturation levels. Typically, undisturbed samples displayed no signs of crystallization for times on the order of days ($\sim 10^5$ s). Upon exposure to brief (~ 10 ns) laser pulses, however, crystallization was often observed. For our purposes, the most important results are that:

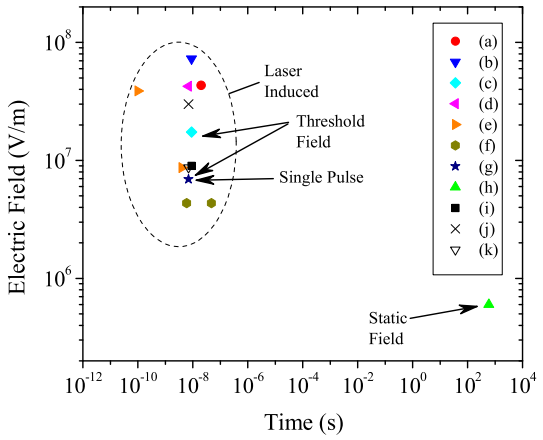

Fig. 4 Summary of NPLIN data in aqueous solutions of: (a) urea;[7] (b) α- and γ- glycine;[8,9] (c) urea;[8] (d) L-histidine;[10] (e) lysozyme;[11] (f) KCl;[12] (g) KCl;[13] (h) γ-glycine.[20] Also shown are nucleation of (i) CO_2 bubbles in water,[17] (j) molten sodium chlorate,[19] and (k) acetic acid.[15] The ordinate is the peak applied field (unless labeled as the threshold field) at which nucleation occurred within the exposure time on the abscissa. The typical laser wavelength was $\lambda = 1.064$ μm, except for (e), (f), and (i) at $\lambda = 0.532$ μm and/or $\lambda = 0.355$ μm. Samples were exposed to numerous laser pulses (except for one case of single pulse exposure[13]) and, typically, less than half of the samples crystallized when irradiated even at the maximum intensity.

(i) the field reduces the nucleation time by 13 orders of magnitude or even more; and
(ii) it can do so at optical frequencies ($\sim 10^{14}$ Hz).
Other observations include:
(iii) the existence of a threshold field, below which nucleation did not occur; and
(iv) a linear-type correlation between the cumulative fraction of samples nucleated and laser intensity,[8,13] as well as the solute supersaturation.[13]

The anomalous strength of the observed field effect can be conveniently expressed in terms of the nucleation barrier, W_0, that determines the nucleus induction time, $\tau = \tau_0 \exp(W_0/kT)$, where $\tau_0 \gtrsim 10^{-13}$ s is the characteristic atomic vibration or diffusion time. The observed reduction of τ by a factor of 10^{-13} requires decreasing the nucleation barrier by approximately $\Delta W(E) = W_0 - W(E) \sim 30kT$. Earlier proposed mechanisms based on the Kerr effect[7] or isotropic atomic polarizability of dielectric clusters[13,14] provided coherent qualitative features but were shown to produce effects on the order of only $10^{-4}kT$, five orders of magnitude below the observations. More recent hypotheses, based on bubble nucleation in carbonated water[17,18] and heterogeneous nucleation in molten salts,[19] leave the causal connection to the electric field undetermined.

That the expected field effect on nucleation is extremely weak compared to NPLIN observations, was fully realized by Alexander et. al.,[13,14] who introduced an adjustable scaling factor of $\sim 10^5$ in order to fit the observed NPLIN data with model based on classical nucleation of dielectric particles. The fitting parameters resulted in an insignificant field induced reduction of the critical radius [cf. Eq. (5)] by $\sim 10^{-4}$ nm. The same conclusion of insufficiency of the known mechanisms of nucleation to explain NPLIN was made recently based on a more quantitative analysis.[17] Furthermore, the predicted dependencies need to be artificially shifted to reproduce the observed threshold in laser power, which cannot be explained by the classical theory. We note that overlooking these problems can lead to the incorrect conclusion that classical nucleation theory can explain the NPLIN observations; some qualitative trends may be compelling but the magnitudes are far too low.

Based on the theory presented here, we consider the possibility that NPLIN of dielectric particles evolves through nucleation of short-lived, needle-shaped, progenitor metallic particles that nucleate under strong electric fields. The concept of solvated electrons could provide a microscopic picture for these precursor metallic nuclei. (A possible side development is that our theory predicts, in principle, the possibility of metallic water under strong enough fields at pressures and temperatures orders of magnitude below the predicted values for zero field.[46]). However, the hypothesis of solvated electrons as the origin of the metallic particles does not have enough supporting data. In particular, the thermodynamic characteristics of nonmetal-metal transitions in systems of solvated electrons remain poorly understood and, to our knowledge, there is no published experimental evidence of the existence of solvated electrons in potassium chloride and similar solutions.

Regardless, it appears that FIN, along with the hypothesis of metallic precursor nuclei, may help to explain the NPLIN data but leaves several open questions. The successes, the remaining questions, and possible experimental methods of verification of this mechanism are summarized in the following subsections.

6.1.1 What is understood

The theory presented here can account for the following NPLIN observations:
1) The abnormally strong reaction to the electric/laser field as provided by the gigantic polarization of metallic, needle-shaped particles. Based on a phenomenological description of such particles, the theory predicts the experimentally observed field range without any adjustment of parameters [cf. Eq. (10) and Fig. 2].
2) The effect of polarization and the appearance of strongly

anisotropic nuclei aligned with the field polarization.
3) Nucleation in response to electric fields of optical frequencies due to the uniquely high plasma frequency of electrons in metals.
4) Existence of a threshold electric field or laser power density above which NPLIN takes place, and independence of that field on such system parameters as the solute over-saturation [cf. Eq. (14)].
5) The observed dc threshold fields an order of magnitude below that of the laser threshold fields due to the significant difference between the static and high frequency dielectric permittivities of the solvent.
6) The number of nucleated particles quadratic in the electric field (linear in laser power) and linear in the solute oversaturation [cf. Eq. (16)].

6.1.2 What is not understood

The following aspects of the theory require further investigation:
1) The microscopic nature of the proposed metallic precursors.
2) The mechanism of transformation from the metallic, needle-shaped particles to the observed dielectric particles that in some cases are needle-shaped, while in others are more isotropic.
3) The scenario of possible shock waves and cavitation following nucleation of metallic particles leading to secondary nucleation of dielectric particles.

6.1.3 Possible experimental verification

We briefly mention possible experimental verifications of our theory.
1) Detecting needle-shaped metallic particles through their characteristic features in light scattering[49] using both the NPLIN-scattered light and an additional probing laser beam. This is described in more detail in the Appendix below.
2) Verifying our prediction that NPLIN will be suppressed under sub-nanosecond laser pulses.
3) Verifying the temperature dependence of the NPLIN product as related to the diffusion coefficient [cf. Eq. (16)].
4) Studying systems with higher concentrations of solvated electrons, particularly generated by low energy X-ray radiation or other extraneous controllable sources.
5) Observing the known characteristic properties of solvated electrons, particularly their spectroscopic features, in parallel with NPLIN experiments.[50–52] More generally, trying to observe new spectral features in absorption and reflection of light under NPLIN conditions.
6) Observing drift of needle-shaped nuclei in an additional *nonuniform* electric field, such as, e.g., created by a conical electrode.
7) Conducting NPLIN experiments in a dc field over a broad range of exposure times to verify the logarithmic time dependence of the threshold field in Eq. (14).

6.1.4 Other considerations

Our proposed theory, while approximate, remains sound at least in the order of magnitude predictions that are all consistent with the observations without adjusting parameters. For example, the ignored dependence of surface tension on particle curvature and on the external field strength cannot lead to qualitatively different predictions. Indeed, neglecting the first factor is not more significant than in the classical nucleation theory where it has been proven to be qualitatively sound, while the second factor can only lead to corrections that are small compared to the ratio of the external field over the characteristic atomic field responsible for the surface tension. Similarly, the concept of classical nucleation theory remains at least semiquantitatively valid as applied to clusters of not too many molecules, say, 10-100 in our case.[48]

6.2 Conclusions

In conclusion, we have presented a theoretical basis for electric field driven nucleation of metals in solutions and other liquid systems. The magnitude of the field effect can be sufficient to nucleate conductive particles that would be unstable in the absence of the field. That mechanism leads to the possibility that NPLIN of dielectric crystals could be preceded by metallic progenitor embryos, especially in the presence of high concentrations of solvated electrons. Another possible application may arise in the laser-induced water condensation in air where a short-lived plasma leads to the final observed dielectric product of water. Broadly speaking, the possibility that detectable metallic clusters can be created by an electric field in overall insulating systems can open a venue of new phenomena with great significance in fundamental understanding and materials technology.

A Optical properties of anisotropic metallic particles

Here we briefly review the characteristic optical features of strongly anisotropic ($H/R \gg 1$) spheroidal metallic particles[53] that can be used to experimentally verify the theory proposed in this work. These features remain one of the hot topics in optical sciences, constituting a field commonly referred to as plasmonics,[34] as related to surface plasmons which are collective oscillations of quasi-free electrons in nanoparticles. The plasmon excitations show up in resonance absorption, scattering, and second harmonic generation. The corresponding cross-sections depend on the dielectric permittivities of the particle and host materials and particle aspect ratio. Multiple consequences include resonant enhancement (up to sev-

eral hundredfold) of the electric field near the particle surface, corresponding anomalies in Raman scattering by tangent molecules, increase in local temperature,[54] and various applications such as nano barcodes, metallic waveguides, lithography, etc.[34,55]

Closed form analytical expressions for the linear optics plasmon-related absorption and scattering by metallic spheroidal particles have been derived.[56,57] In particular, the differential scattering cross-section by the high aspect ratio spheroidal metallic particles[56] can be presented in our notation as,

$$\frac{d\Sigma}{d\Omega} = \frac{\varepsilon^2 V^2 \omega^4 \sin^2\theta}{16\pi^2 c^4}\left[\frac{\Phi_{\|}\cos^2\phi}{n^2} + 4\Phi_{\perp}\sin^2\phi\right] \qquad (17)$$

where Ω is the solid angle, ω is the light frequency, ω_p is the plasmon frequency, c is the speed of light, θ and ϕ are the polar and azimuthal angles, the depolarizing factor $n \sim (R/H)^2 \ll 1$ is defined in Eq. (6), and $\Phi_{\|}$ and $\Phi_{\perp}$ are the frequency dependent resonance factors related to the long and short axes of a spheroidal particle respectively,

$$\Phi_{\|} = \frac{1}{n^2}\frac{[n(1-\varepsilon^{-1})\omega^2 + \omega_p^2]^2 + (4\pi n\sigma_{\|}\omega/\varepsilon)^2}{(\omega^2 - \omega_p^2 n)^2 + (4\pi n\sigma_{\|}\omega/\varepsilon)^2},$$

$$\Phi_{\perp} = \frac{[\omega^2/2 - \omega_p^2(1+\varepsilon)^{-1}]^2 + (4\pi\sigma_{\perp}\omega/(1+\varepsilon))^2}{(\omega^2 - \omega_p^2(1+\varepsilon)^{-1})^2 + (4\pi\sigma_{\perp}\omega/(1+\varepsilon))^2}.$$

Here the principal components of the conductivity tensor, $\sigma_{\|}$ and $\sigma_{\perp}$, are different if the electron mean free path is shorter than the particle radius R, in which case it was estimated that,

$$\sigma_{\|} = \left(\frac{3}{16}\right)^2\left(\frac{\omega_p}{\omega}\right)^2\frac{v_F}{R}, \quad \sigma_{\perp} = 1.5\sigma_{\|}, \qquad (18)$$

where v_F is the Fermi velocity.

The above scattering spectrum exhibits two peaks corresponding to plasmonic excitations parallel to the short and long axes of the metallic spheroidal particle. The low frequency peak at $\omega \approx \omega_p\sqrt{n} \approx \omega_p(R/H)$, likely in the near-infrared, shifts with the particle aspect ratio; this peak is relatively narrow as its width is suppressed by the same factor $R/H \ll 1$. The high frequency peak, at $\omega \approx \omega_p/\sqrt{1+\varepsilon}$, likely in the visible spectrum, is almost independent of particle dimensions and is much broader. These and other predictions are in general agreement with observations on metallic nanorods.[58,59]

Nonlinear optical properties of the predicted anisotropic nanoparticles lead to very efficient second harmonic generation that can be used for verification purposes. This effect has a resonance nature as well increasing drastically at $\omega_p/2$ and $\omega_p/2\sqrt{2}$. The high-frequency resonance is induced mostly by light with polarization parallel to the particle short axis, while the low-frequency resonance is caused by light with polarization parallel to the long axis. Spatial distribution and polarization of the second harmonic emitted light are different for the two resonances.[60]

References

1 V. G. Karpov, Y. A. Kryukov, I. V. Karpov, and M. Mitra, *Phys. Rev. B*, 2008, **78**, 052201; I. V. Karpov, M. Mitra, G. Spadini, U. Kau, Y. A. Kryukov, and V. G. Karpov, *Appl. Phys. Lett.*, 2008, **92**, 173501; M. Nardone, V. G. Karpov, C. Jackson, and I. V. Karpov, *ibid.*, 2009, **94**, 103509.

2 M. Nardone and V. G. Karpov, *Appl. Phys. Lett.*, 2012, **100**, 151912.

3 V. G. Karpov, *Appl. Phys. Lett.*, 2010, **97**, 033505.

4 A. Madan and M.P. Shaw, *The Physics and Applications of Amorphous Semiconductors*, Academic Press, San Diego, 1988.

5 Y. Hirose and H. Hirose, *J. Appl. Phys.*, 1976, **47**, 2767–2772.

6 A. B. Pevtsov, A. V. Medvedev, D. A. Kurdyukov, N. D. Il'inskaya, V. G. Golubev, and V. G. Karpov, *Phys. Rev. B*, 2012, **85**, 024110.

7 B. A. Garetz, J. E. Aber, N. L. Goddard, R. G. Young, and A. S. Myerson, *Phys. Rev. Lett.*, 1996, **77**, 3475–3476.

8 B. A. Garetz, J. Matic, and A. S. Myerson, *Phys. Rev. Lett.*, 2002, **89**, 175501.

9 J. Zaccaro, J. Matic, A. S. Myerson, and B. A. Garetz, *Cryst. Growth Des.*, 2001, **1**, 5–8.

10 X. Sun, B. A. Garetz, and A. S. Myerson, *Crys. Growth Des.*, 2008, **8**, 1720–1722.

11 I. S. Lee, J. M. B. Evans, D. Erdemir, A. Y. Lee, B. A. Garetz, and A. S. Myerson, *Crys. Growth Des.*, 2008, **8**, 4255–4261.

12 M. R. Ward, I. Ballingall, M. L. Costen, K. G. McKendrick, and A. J. Alexander, *Chem. Phys. Lett.*, 2009, **481**, 25–28.

13 A. J. Alexander and P. J. Camp, *Crys. Growth Des.*, 2009, **9**, 958–963.

14 C. Duffus, P. J. Camp, and A. J. Alexander, *J. Am. Chem. Soc.*, 2009, **131**, 11676–11677.

15 M. R. Ward, S. McHugh and A. J. Alexander, *Phys. Chem. Chem. Phys.*, 2012, **14**, 90–93.

16 X. Sun, B. A. Garetz, M. F. Moreira, and P. Palffy-Muhoray, *Phys. Rev. E*, 2009, **79**, 021701.

17 B. C. Knott, J. L. LaRue, A. M. Wodtke, M. F. Doherty, and B. Peters, *J. Chem. Phys.*, 2001, **134**, 171102.

18 B. C. Knott, M. F. Doherty, and B. Peters, *J. Chem. Phys.*, 2011, **134**, 154501.

19 M. R. Ward, G. W. Copeland, and A. J. Alexander, *J. Chem Phys.*, 2001, **135**, 114508.

20 J. E. Aber, S. Arnold, B. A. Garetz, and A. S. Myerson, *Phys. Rev. Lett.*, 2005, **94**, 145503.

21 D. W. Oxtoby, *Nature*, 2002, **420**, 277–278.

22 P. Rohwetter, J. Kasparian, K. Stelmaszczyk, Z. Hao, S. Henin, N. Lascoux, W. M. Nakaema, Y. Petit, M. Queiszer, R. Salame, E. Salmon, L. Woste, and J. P. Wolf, *Nat. Photonics*, 2010, **4**, 451–456.

23 R. C. deVekey and A. J. Majumdar, *Nature*, 1970, **225**, 172–173; W. Liu, K. M. Liang, Y. K. Zheng, S. R. Gu, H. Chen, *J. Phys. D: Appl. Phys.*, 1997, **30**, 3366–3370; J. Duchene, M. Terraillon, P. Paily, and G. Adam, *Appl. Phys. Lett.*, 1971, **19**, 115–117; B.-J. Kim, Y. W. Lee, B.-G. Chae, S. J. Yun, S.-Y. Oh, and H.-T. Kim, *Appl. Phys. Lett.*, 2007, **90**, 023515; K. Okimura, N. Ezreena, Y. Sasakawa, and J. Sakai, *Japan J. Appl. Phys.*, 2009, **48**, 065003.

24 V. Lyubin, M. Klebanov, M. Mitkova, and T. Petkova, *Appl. Phys. Lett.*, 1997, **71**, 2118–2120.

25 V. Lyubin, M. Klebanov, and M. Mitkova, *Appl. Surf. Sci.*, 2000, **154-155**, 135–139.

26 A. A. Baganich, V. I. Mikla, D. G. Semak, A. P. Sokolov, and A. P. Shebanin, *Phys. Stat. Sol. (b)*, 1991, **166**, 297–302; V.I. Mikla, I.P. Mikhalko, and V.V. Mikla, *Materials Science and Engineering: B*, 2001, **83**, 74–78.

27 L. D. Landau and E. M. Lifshitz, *Statistical Physics*, 3rd edn, Pergamon, Oxford, 1980.

28 D. Kaschiev, *Cryst. Res. Technol.*, 2003, **38**, 555–574.

29 L. D. Landau, I. M. Lifshitz, and L. P. Pitaevskii, *Electrodynamics of Continuous Media*, Pergamon, Oxford, 1984.

30 D. R. Lide, Ed. *Handbook of Chemistry and Physics, 88th ed.*, CRC Press, Boca Raton, 2007.

31 N. Mott, *Metal-Insulator Transitions* – 2nd edn, Taylor and Francis Ltd., London, 1990.

32 C. G. Garton and Z. Krasucki, *Proc. R. Soc. London, Ser. A*, 1964, **280**, 211–226; V. S. Vorob'ev and S. P. Malyshenko, *JETP*, 2001, **93**, 753–759 [*Zh. Eksper. Teor. Fiz.*, 2001, **120**, 863–869].

33 V. G. Karpov, M. Nardone, and N. I. Grigorchuk, *unpublished*; http://arxiv.org/abs/1205.3988.

34 S. A. Maier, *Plasmonics: Fundamentals and Applications*, Springer, New York, 2007.

35 W. J. Wang, L. P. Shi, R. Zhao, K. G. Lim, H. K. Lee, T. C. Chong, and Y. H. Wu, *Appl. Phys. Lett.*, 2008, **93**, 043121.

36 E. M. Lifshitz and L. P. Pitaevskii, *Physical Kinetics*, Elsevier, Amsterdam, 2008.

37 D. Erdemir, A. Y. Lee, and A. S. Myerson, *Acc. Chem. Res.*, 2009, **42**, 621–629.

38 A. Soare, R. Dijkink, M. R. Pascual, C. Sun, P. W. Cains, D. Lohse, A. I. Stankiewicz, and H. J. M. Kramer, *Crys. Growth Des.*, 2011, **11**, 2311–2316.

39 M. I. Kozlovskii, *Growth of Crystals*, Consultants Bureau, New York, 1966, Vol. 4, p. 20.

40 H. L. Skriver and N. M. Rosengaard, *Phys. Rev. B* , 1992, **46**, 7157–7168.

41 I. Anusiewicz, J. Berdys, J. Simons, and P. Skurski, *J. Chem. Phys.*, 2003, **119**, 902–908.

42 B. Abel and K. R. Siefermann, *Angew. Chem. Int. Ed.*, 2011, **50**, 5264–5272; B. Abel, U. Buck, A. L. Sobolewskic, and W. Domcked, *Phys. Chem. Chem. Phys.*, 2012, **14**, 22–34.

43 J. M. Herbert and L. D. Jacobson, *Int. Rev. Phys. Chem.*, 2011, **30**, 1–48.

44 G. N. Chuev, P. Quicimerais, J. Crain, *J. Chem. Phys.*, 2007, **127**, 244501.

45 U. Schindewolf and M. Werner, *J. Phys. Chem.*, 1980, **84**, 1123–1129.

46 T. R. Mattsson and M. P. Desjarlais, *Phys. Rev. Lett.*, 2006, **97**, 017801.

47 D. H. Son, P. Kambhampati, T. W. Kee, and P. F. Barbara, *J. Phys. Chem. A*, 2001, **105**, 8269–8272.

48 I. M. Lifstitz and Yu. Kagan, *Zh. Eksp. Teor. Fiz.*, 1972, **62**, 385–393 [*Sov. Phys. JETP*, 1972, **35**, 206–214].

49 C. F. Bohren and D. R. Huffman, *Absorption and Scattering of Light by Small Particles*, Wiley, New York, 1983.

50 A. Hertwig, H. Hippler, and A.-N. Unterreiner, *Phys. Chem. Chem. Phys.*, 1999, **1**, 5633–5642.

51 D. M. Bartels, K. Takahashi, J. A. Cline, T. W. Marin, and C. D. Jonah, *J. Phys. Chem. A*, 2005, **109**, 1299–1307.

52 Y. Muroya, M. Lin, Z. Han, Y. Kumagai, A. Sakumi, T. Ueda, and Y. Katsumura, *Radiat. Phys. and Chem.*, 2008, **77**, 1176–1182.

53 *Light Scattering by Nonspherical Particles: Theory, Measurements, Applications*, edited by M. I. Mishchenko, J. W. Hovenier, and L. D. Travis, Academic Press, London, 2000.

54 G. V. Hartland, *Annu. Rev. Phys. Chem.*, 2006, **57**, 403–430.

55 *Surface Plasmon Nanophotonics*, edited by M. L. Brongersma and P. G. Kik, Springer, New York, 2007.

56 N. I. Grigorchuk, Europhys. Lett., 2012, **97**, 45001.

57 P. M. Tomchuk and N. I. Grigorchuk, *Phys. Rev. B*, 2006, **73**, 155423.

58 J. Zhang, L. Zhang, and W. Xu, *J. Phys. D: Appl. Phys.*, 2012, **45**, 113001.

59 E.-A. You, W. Zhou, J. Yong Suh, M. D. Huntington, and T. W. Odom, *ACS Nano*, 2012, **6**, 1786–1794.

60 H. E. Ruda and A. Shik, *J. Appl. Phys.*, 2007, **101**, 034312.

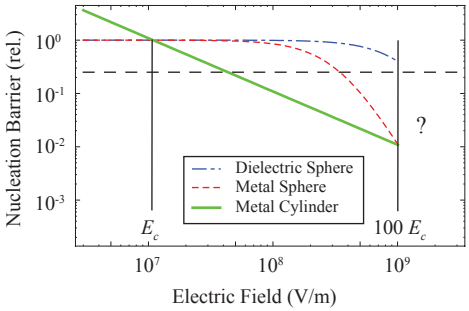

Electric field driven phase transitions can occur via nucleation of elongated, metallic embryos even when the metal phase is unstable.